Effects of torsion frequencies on rotor performance and structural loads with trailing edge flap

2012 Smart Mater. Struct. 21 085026

(http://iopscience.iop.org/0964-1726/21/8/085026)

Report Documentation Page

Form Approved OMB No. 0704-0188

2012		**00-00-2012 to 00-00-2012**

Effects Of Torsion Frequencies On Rotor Performance And Structural Loads With Trailing Edge Flap

a

b

c

( )

d

e

f

( ) ( )

US Army Research, Development, and Engineering Command,Aeroflightdynamics Directorate (AMRDEC),Ames Research Center,Moffett Field,CA,94035

( ) ( )

( )

( )

Approved for public release; distribution unlimited

Smart Materials And Structures, 21 (2012) 085026, 11 June 2012

The effects of variation of blade torsion frequency on rotor performance and structural loads are investigated for a 1=rev active flap rotor and baseline rotor (no active control). The UH-60A four-bladed articulated main rotor is studied at a high-speed forward flight condition. The torsion frequencies are varied by modifying the spanwise torsional stiffness of the blade and/or the pitch link stiffness. First, a parametric/optimization study on the flap deployment schedule is carried out using lifting-line comprehensive analysis for the soft, baseline, and stiff rotor configurations, and then a higher fidelity coupled computational fluid dynamics?computational structural dynamics analysis is carried out for the optimal flap deployment. It is shown that with the soft rotor there is degradation in performance?of about 6% with respect to the baseline rotor in the case where the flaps are not activated, and of about 1% if flap deflections are applied. On the other hand, for the stiff rotor there is a slight improvement in performance of about 2.3% when the flaps are not activated, and no appreciable change in the case where active flap deflections are applied. It appears that the peak performance achievable with using active flaps on a baseline stiffness rotor cannot be further improved significantly by varying the torsional frequencies. Variation of torsion frequency does not appear to have a significant influence on blade torsion moments and pitch link loads, although the 1/rev flap activation examined has an important role.

					a
a **unclassified**	b **unclassified**	c **unclassified**	**Same as Report (SAR)**	**13**	

Smart Mater. Struct. **21** (2012) 085026 (11pp) doi:10.1088/0964-1726/21/8/085026

Effects of torsion frequencies on rotor performance and structural loads with trailing edge flap

Rohit Jain and Hyeonsoo Yeo

Aeroflightdynamics Directorate (AMRDEC), US Army Research, Development, and Engineering Command, Ames Research Center, Moffett Field, CA, USA

E-mail: rjain@merlin.arc.nasa.gov

Received 1 February 2012, in final form 11 June 2012
Published 24 July 2012
Online at stacks.iop.org/SMS/21/085026

Abstract
The effects of variation of blade torsion frequency on rotor performance and structural loads are investigated for a 1/rev active flap rotor and baseline rotor (no active control). The UH-60A four-bladed articulated main rotor is studied at a high-speed forward flight condition. The torsion frequencies are varied by modifying the spanwise torsional stiffness of the blade and/or the pitch link stiffness. First, a parametric/optimization study on the flap deployment schedule is carried out using lifting-line comprehensive analysis for the soft, baseline, and stiff rotor configurations, and then a higher fidelity coupled computational fluid dynamics–computational structural dynamics analysis is carried out for the optimal flap deployment. It is shown that with the soft rotor there is degradation in performance—of about 6% with respect to the baseline rotor in the case where the flaps are not activated, and of about 1% if flap deflections are applied. On the other hand, for the stiff rotor there is a slight improvement in performance of about 2.3% when the flaps are not activated, and no appreciable change in the case where active flap deflections are applied. It appears that the peak performance achievable with using active flaps on a baseline stiffness rotor cannot be further improved significantly by varying the torsional frequencies. Variation of torsion frequency does not appear to have a significant influence on blade torsion moments and pitch link loads, although the 1/rev flap activation examined has an important role.

(Some figures may appear in colour only in the online journal)

Nomenclature

C	blade chord, inch
C^{TED}	TED chordwise width, percentage of C
C_{T}	rotor thrust coefficient
D_{e}	rotor effective drag
F_{p}	rotor propulsive force
GJ	blade torsional stiffness
L	rotor lift
L/D_{e}	rotor lift to effective drag ratio, $L/(P/V - F_{\mathrm{p}})$
M	blade section local Mach number
M^2C_{D}	blade section force component in the rotor disk plane in tangential direction (non-radial component)
M^2C_{L}	blade section force component normal to the rotor disk plane
P	rotor power
PL	pitch link stiffness
R	rotor radius
$R_{\mathrm{TED}}^{\mathrm{inner}}$	TED inner span, % of R
$R_{\mathrm{TED}}^{\mathrm{outer}}$	TED inner span, % of R
TED	trailing edge deflection
V	rotor forward speed
δ^{TED}	TED amplitude, degree
σ	rotor solidity
ψ	rotor azimuth angle. Wind direction is left to right and rotor rotates in a counterclockwise direction. Zero degrees azimuth is aft, 90° is advancing side, and so on.

1. Introduction

Next generation rotorcraft require a significant increase in speed, range, and payload capabilities. Active rotor control technologies [1] have shown the potential to meet the requirements of a next generation rotorcraft. Many active rotor control research efforts have attempted to distribute the lift and drag around the rotor disk to achieve a net power reduction by modifying the rotor blade pitch at proper harmonic frequencies and phase angles. Active rotor technology examples include individual blade control using hydraulically actuated pitch links [2–7], active twist rotor using piezoelectric active fiber composite technology [8–10], and trailing edge flaps [11–15]. The trailing edge flap provides blade pitch change indirectly. Deflection of a trailing edge flap alters the camber of the blade section and changes its aerodynamics characteristics. The flap functions as a moment flap as the change in the airfoil's pitching moment characteristics has the most crucial effect which causes the blades to pitch. However, at higher torsion stiffness of rotor blades, the effectiveness of a moment flap diminishes and the flap functions largely as a lift flap.

The effectiveness of such on-blade active control is sensitive to the blade torsion frequencies. Previous studies showed that torsionally soft blades were more effective in vibration reduction and primary control applications (swashplateless rotor) [16, 17]. The design and development of active blades requires careful selection of blade torsion frequencies which produce good baseline (no active control) rotor performance and at the same time provide sufficient control authority. A previous investigation (based on comprehensive analysis and coupled computational fluid dynamics (CFD)–computational structural dynamics (CSD) analysis) of an active rotor with trailing edge deflection (TED) showed that at high-speed forward flight, TED enhances the rotor aerodynamic efficiency by generating positive (nose up) pitching moments which twist the blade nose up in the negative lift region on the advancing side and generate lift without an associated drag increase [18]. Since the twisting of the blade caused by aerodynamic pitching moments is the key mechanism here, the torsional stiffness of the blade is a key parameter affecting the authority of aerodynamic moments.

The current study investigates the effects of blade torsion frequencies on rotor performance improvement of a four-blade articulated rotor with trailing edge flaps using a coupled CFD–CSD analysis. The objectives are to quantify the effects of blade torsion frequencies on rotor performance at high-speed steady-level flight and understand the physics behind it.

2. Approaches

The baseline rotor studied in this paper is the UH-60A main rotor. The rotor blade parameters are listed in table 1. The high-speed steady-level forward flight condition (flight counter c8534 of the NASA/Army UH-60A Airloads Program in [19]) is chosen to examine the effects of blade torsion frequencies on rotor performance with trailing edge flap. This high-speed flight is characterized by transonic flow on the advancing side which causes high vibratory hub loads. The flight condition is listed in table 2.

Table 1. UH-60A blade parameters.

Parameter	Value
Number of blades	4
Radius (R), in	322
Mean chord (C), in	20.76
Thickness, % chord	9.5/9.4
Rotor disk area, ft^2	2261.5
Rotor blade area, ft^2	186.9
Solidity ratio	0.0826
Blade tip sweep, aft, deg.	20
Airfoils	SC1095/SC1094R8
Nominal rotor speed, Ω, rpm	258
First torsional frequency, /rev	4.53
Pre-twist, deg.	−18, nonlinear

Table 2. UH-60A high-speed forward flight conditions (c8534) [19].

Parameter	Value
Density, slug ft^{-3}	0.002 0823
Temperature, $^\circ$F	71.8
Rotor speed, rpm	258.1
Airspeed, ft s^{-1}	266
Advance ratio, μ	0.36
Blade loading, C_T/σ	0.084
Freestream mach	0.236

The baseline rotor blade frequencies were calculated in vacuum using the comprehensive analysis code, RCAS [20] and plotted as a function of the normalized rotor speed in figure 1(a). The frequencies shown here are for a 14° collective pitch with a very small structural damping. The labeling of the modes corresponds to the nominal rotor speed of 258 rpm. There are strong couplings between modes for third to fifth modes. At the nominal rotor speed, the fourth mode is predominantly a torsion mode and the frequency is 4.53/rev.

Soft and stiff rotor configurations considered in this study are obtained by changing the structural properties of the baseline rotor mentioned above. The soft rotor configuration is obtained by uniformly reducing the torsional stiffness (GJ) of the entire span of the rotor blade and/or reducing the stiffness of the pitch link. Stiff rotor configurations are obtained by increasing the GJ above the baseline values. Figures 1(b) and (c) show the blade frequencies for one soft blade case (50%GJ) and one stiff blade case (150%GJ), respectively. For the soft case, the first torsion frequency was reduced below 4/rev and thus the torsion mode was further separated from the second lag mode and moved closer to the second flap mode. For the stiff case, the first torsion frequency increased above 5/rev, between second lag and third flap mode at the nominal rpm. The first torsional frequencies at the nominal rpm of all the soft and stiff rotor configurations studied here are shown in table 3.

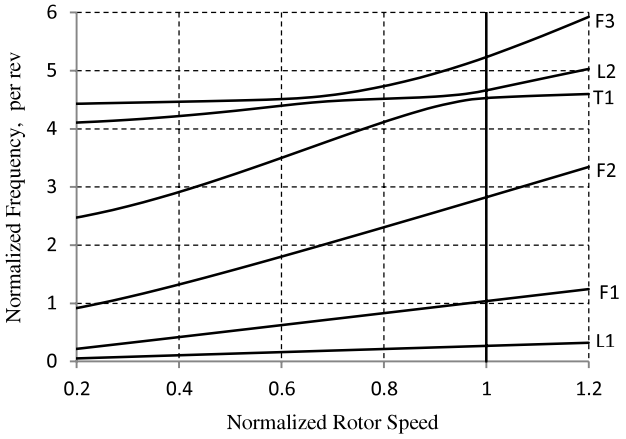

(a)

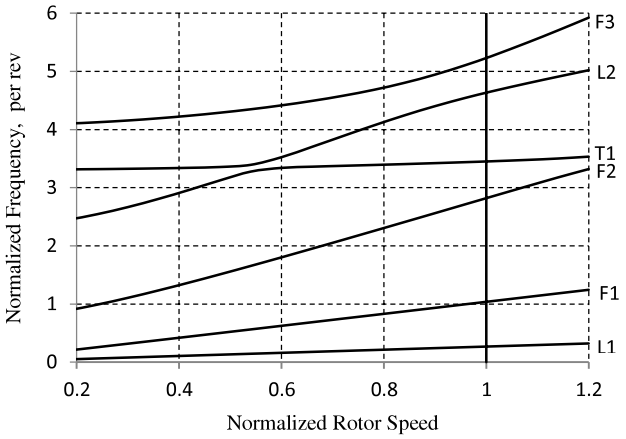

(b)

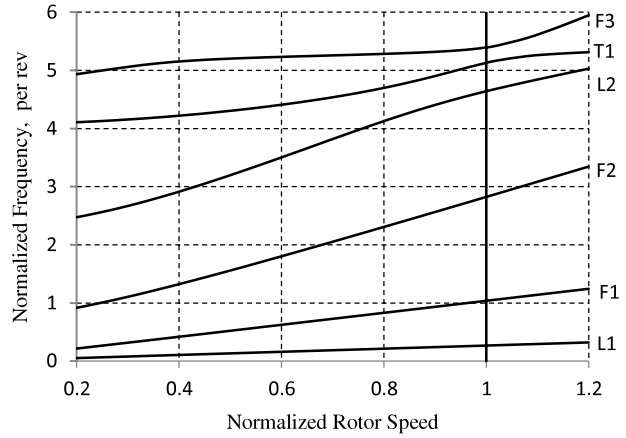

(c)

Figure 1. Rotor natural frequencies in vacuum computed using RCAS. The collective angle is 14°. (a) 100%GJ, (b) 50%GJ, and (c) 150%GJ.

3. Simulation setup

Two approaches have been taken in the numerical analysis—(1) lifting-line comprehensive analysis and (2) coupled CFD–CSD analysis. The former approach typically uses an aerodynamics model based on conventional lifting-line theory and a vortex wake model to calculate the rotor non-uniform induced velocities. Airfoil tables in C81 format are used to obtain section lift, drag, and pitching moment for the section angle of attack and Mach number. This approach is computationally efficient, and is especially suitable for use in initial exploration of design spaces in rotor optimization problems. The latter approach (CFD–CSD) is a more rigorous, higher fidelity modeling of the rotor aerodynamics by numerically solving the full 3D Reynolds averaged Navier–Stokes (RANS) equations based on CFD. CFD is coupled with CSD to obtain high fidelity aerodynamics and structural modeling of the rotor.

Table 3. Torsional frequency of the soft, nominal, and stiff rotor configurations.

Torsional stiffness[a]	Pitch link stiffness[a]	Torsional frequency[b], /rev	
50	33	3.20	Soft
50	100	3.45	Soft
100	33	3.95	Soft
100	100	4.53	Nominal
125	100	4.93	Stiff
150	100	5.14	Stiff

[a] Percentage of the baseline rotor.

[b] In vacuum, at nominal rotor speed of 258 rpm.

In this study RCAS has been used for lifting-line comprehensive analysis. For coupled CFD–CSD analysis, the CFD code WIND-US-HELI [21, 22] has been used and it is coupled with RCAS for the modeling of structural dynamics. RCAS and WIND-US-HELI are coupled using the standard 'delta-formulation' technique [23–26]. Coupling iterations are carried out wherein RCAS and WIND-US-HELI are executed in sequence exchanging data once per rotor period (referred to as loose-coupling). A coupling iteration consists of one CSD step wherein RCAS computes blade deflections using the CFD airloads from the previous coupling iteration, and one CFD step wherein WIND-US-HELI computes a new set of blade airloads using the blade deflections. The coupling iterations are carried out until the airloads are converged. In the delta-formulation technique, the CFD airloads are applied in the form of a delta correction to RCAS. The delta correction is the difference between the CFD airloads and the lifting-line airloads obtained from RCAS from the previous coupling iteration. Therefore, during the RCAS simulation, RCAS computes and applies lifting-line airloads to the blade and, in addition, the delta correction airloads are applied as external forces and moments on the blades. Upon convergence, the lifting-line airloads from the current iteration cancel out the lifting-line airloads from the previous iteration and, in effect, only the CFD airloads get applied in RCAS. The coupled analysis of RCAS and WIND-US-HELI was validated in [21] for the UH-60A rotor (without a trailing edge flap) at the same high-speed flight condition investigated here.

Under previous studies [18, 27], several trailing edge flap deployment strategies—including harmonic deployments over a wide range of amplitude, phase angle, and frequency, and a few non-harmonic deployments—were investigated for the baseline rotor. The geometric parameters for TED are shown in figure 2. It was found that both a harmonic 1/rev deployment at 90° phase angle ($\delta^{\mathrm{TED}} = A\cos(\psi +$

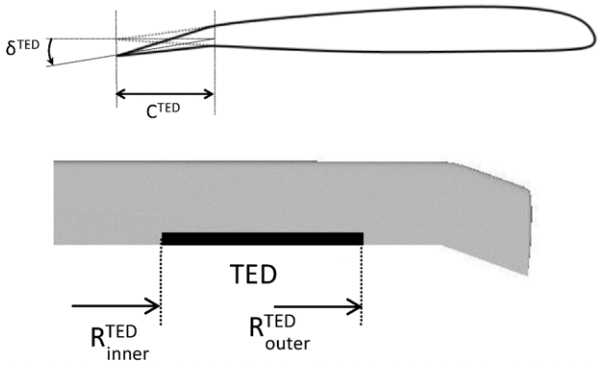

Figure 2. Trailing edge deflection (TED) parameters.

90) degrees) and a non-harmonic deployment strategy (with a δ_{TED} of $-2.6°$ and $+6.6°$ on the advancing and retreating sides, respectively) resulted in the best performance (rotor L/D_{e}) gains. The next largest gain was seen with a 2/rev harmonic deployment at 0° phase angle.

In order to investigate the effects of torsion frequencies on rotor performance, the 1/rev deployment is selected for the present study. The TED inner and outer radial span, $R^{\text{TED}}_{\text{inner}}$ and $R^{\text{TED}}_{\text{outer}}$ are $67\%R$ and $87\%R$ respectively, and chordwise width, C^{TED} is $20\%C$. The structural properties of the blade are not modified to account for the flap system. In practice, the structural properties of the rotor will change as a result of installation of the flap system onto the rotor. However, the basic characteristics of the rotor system studied here i.e. the effect of variation of torsional stiffness on rotor performance, are fundamental in nature, and are expected to remain applicable to the flapped rotor system with modified structural properties. As mentioned before, in order to obtain torsionally soft or stiff rotor configurations, the torsional stiffness of the rotor is uniformly modified for the entire rotor span. Also, the structural twist of the rotor is not modified as the blade stiffness is changed. The performance of the soft and stiff rotors might be improved by re-optimizing the twist distribution as a function of the stiffness. However, in the present study the structural twist of the baseline rotor is used for all of the soft, baseline, and stiff rotor cases.

4. Performance analysis with RCAS

An initial, exploratory parametric study was carried out using comprehensive analysis RCAS with lifting-line aerodynamics and free-wake inflow model. For each soft and stiff rotor configuration of table 3, the effect of the variation of amplitude and phase of 1/rev TED deployment on rotor performance (rotor L/D_{e}) was computed. The amplitude was varied from 0° to 4° in increments of 0.5°, and for each amplitude, the phase angle was varied from 0° to 300° in increments of 60°. Additionally, the 90° phase angle is considered, as it was shown in the previous studies that the performance improvement for the baseline rotor was maximum at this phase angle for a given amplitude. In each simulation the rotor was re-trimmed using a propulsive trim strategy. The trim state of the rotor was specified in terms of

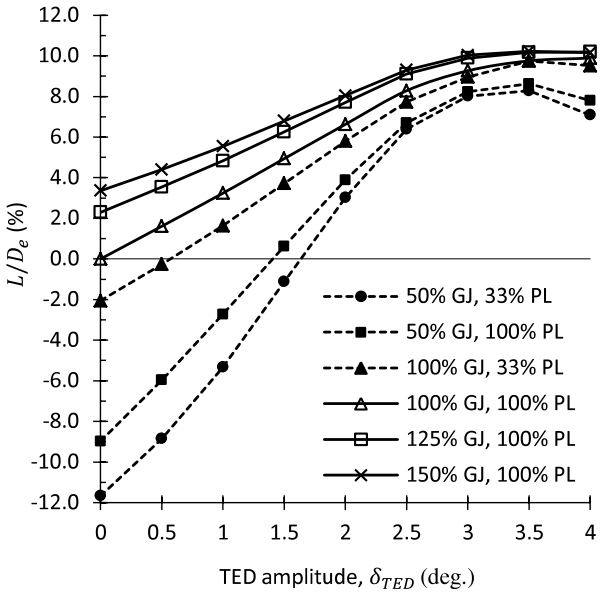

Figure 3. Rotor performance with respect to the baseline rotor (100% GJ, 100% PL, and no TED) for torsionally stiff and soft rotors, computed using lifting-line comprehensive analyses.

the following trim targets: rotor lift, hub pitching and rolling moments, and propulsive force, and the trim variables were collective pitch angle, lateral cyclic pitch angle, longitudinal cyclic pitch angle, and (hub) shaft tilt angle.

The comprehensive analysis results showed that for all the rotor stiffness values and for all TED amplitudes examined in the present study, the maximum performance was again achieved at the 90° phase angle. Therefore, the rotor performance variation with respect to the baseline rotor ($100\%GJ$ and no TED) at the 90° phase angle as a function of TED amplitude is shown for the baseline, soft, and stiff rotors in figure 3. Consider first the case where the amplitude is zero (no TED). The figure shows that there is a significant variation in the rotor performance with variation of the blade torsional stiffness and thus blade torsional frequencies. As the torsional frequency reduces (softness increases), there is a higher penalty in rotor performance. For the lowest torsional frequency of 3.2/rev considered here, the penalty is about 12.0%. To gain back the baseline rotor performance, a TED amplitude of about 1.5° is required. On the other hand, for the stiff rotors there is a gain in performance. For the stiffest rotor of torsional frequency at 5.14/rev considered here, the gain in rotor performance is about 3.0%.

In the case of 1/rev TED, as the TED amplitude is increased the rotor performance generally improves. The performance improvement peaks at approximately 3.5°. The performance improvement with 3° amplitude for the baseline rotor stiffness is about 9.3%, for the softest rotor is 8.0%, and for the stiffest rotor is 10.0%.

Thus, in the case of no TED (TED amplitude of 0° in figure 3), there is a significant variation in the rotor performance from -12.0% (penalty) in the case of the softest rotor to $+3.0\%$ (gain) in the case of the stiffest rotor. However, in the case of TED, the change in peak rotor performance is relatively small—the peak performance changes from 8.0%

in the case of the softest rotor to 9.3% in the case of baseline stiffness to 10.0% in the case of the stiffest rotor. Thus, the reduction in peak rotor performance is only about 1.3% from baseline to the softest rotor and gain is only about 0.7% from baseline to the stiffest rotor. It is noted that the soft rotor shows a large improvement relative to its own baseline (soft rotor, no TED)—the performance gain is about 20%. On the other hand, the stiff rotor shows a relatively small improvement with respect to its own baseline (stiff rotor, no TED)—the performance gain is about 7%.

5. Performance analysis with CFD/CSD

The results shown in section 4 were obtained from the comprehensive analysis. The key mechanism responsible for the improved performance using TED is the counteraction of nose down unsteady transonic pitching moments on the advancing side by deploying a negative (upward) TED on the advancing side [18]. Since the unsteady transonic flow aerodynamics is not well captured by comprehensive analysis, which uses airfoil look-up tables for computing the airloads, more detailed examinations on rotor performance (rotor L/D_e) and loads were carried out using coupled CFD–CSD analysis. First, conclusions drawn using the comprehensive analysis were verified against higher fidelity solutions for select cases and then detailed aerodynamics were examined to better understand the physics. Soft (50%GJ), baseline (100%GJ), and stiff (150%GJ) rotors with the pitch link stiffness of the baseline rotor are considered without and with TED. The TED frequency is 1/rev, amplitude is 3°, and phase angle is 90°.

The computed rotor performance with respect to the baseline rotor without TED is shown in figure 4. Consistent with the comprehensive analysis predictions, the coupled CFD–CSD analysis also predicts a degradation in performance of the soft rotor without and with TED—without TED the performance degrades from 0% (baseline rotor) to −6.2% (soft rotor), and with TED the performance degrades from +7.8% (baseline rotor) to 6.7% (soft rotor). In the case of a stiff rotor without TED, the performance improves from 0.0% to 2.3%, showing a trend consistent with the comprehensive analysis results. Finally, in the case of a stiff rotor with TED, the CFD–CDS analysis predicts a small decrease in performance from +7.8% (baseline rotor) to +7.5% (soft rotor) while the comprehensive analysis predicts a small increase from +9.3% to 10.0%.

In order to better understand the effects of torsion frequency on the rotor performance, detailed aerodynamics on the rotor disk are examined for the next couple of figures. Figure 5 shows the calculated rotor blade sectional lift and drag with the coupled analysis for the soft blade without TED. The top row shows the baseline (100% GJ) results, the second row shows the results obtained with the 50% GJ, and the third row shows the difference between the two results. The figure shows that there is a loss of lift on the front and aft of the rotor disk which is redistributed as an increase on the outboard of the retreating side and inboard of the advancing side. There is a corresponding decrease/increase of drag. The increase in

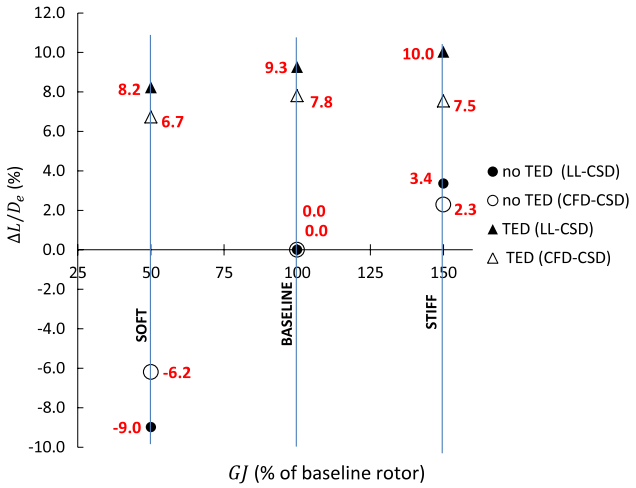

Figure 4. Effect of the rotor torsional stiffness on the relative rotor performance, computed using lifting-line comprehensive analysis and coupled CFD–CSD analysis.

drag on the outboard of the retreating side appears to be of higher magnitude than the decrease seen on the outboard of the front and aft side, and the combined changes in lift and drag cause the calculated decrease in performance. Figure 6 shows the calculated rotor blade sectional lift and drag with the coupled analysis for the soft blade with 1/rev TED. The lift distribution on the rotor disk shows that application of 1/rev TED with 3° amplitude and 90° phase creates additional lift on the outboard region of the advancing side, and there does not seem to be a corresponding increase in drag. Note that the aerodynamic efficiency of the rotor has increased for both baseline (100% GJ) and soft (50% GJ) cases. In [18], it was shown that this was the key mechanism in improving the rotor performance in high-speed flight conditions using TED. For the soft rotor this mechanism is further enhanced possibly due to the increased authority of TED in inducing oscillatory (1/rev) pitch in the blade. In order to maintain the roll trim, lift on the retreating side also increases via an increase in the collective angle and a decrease in the longitudinal angle. The drag also increases on the retreating side. In order to maintain the trim condition on lift, the lift on the front and aft decreases, and, correspondingly, the drag also decreases. Overall the performance of the soft rotor degrades primarily due to the increase in drag over the retreating side.

The rotor disk loading for the stiff rotor without TED is shown in figure 7. The loading is shown with respect to the case of baseline stiffness (100% GJ) without TED. There is an increase in lift on the outboard of the advancing side around 130° azimuth. The stiff rotor undergoes less of a nose down pitching due to the unsteady transonic pitching moments on the advancing side, compared to the baseline rotor. A reduction in nose down pitch causes the airfoil to operate more efficiently and hence additional lift is created without any significant accompanying drag. The hub moment trim condition causes the lift to be increased in the diametrically opposite region, and the lift trim condition causes the lift to be decreased on the retreating side around 200° azimuth and on the inboard region of the advancing side. Correspondingly

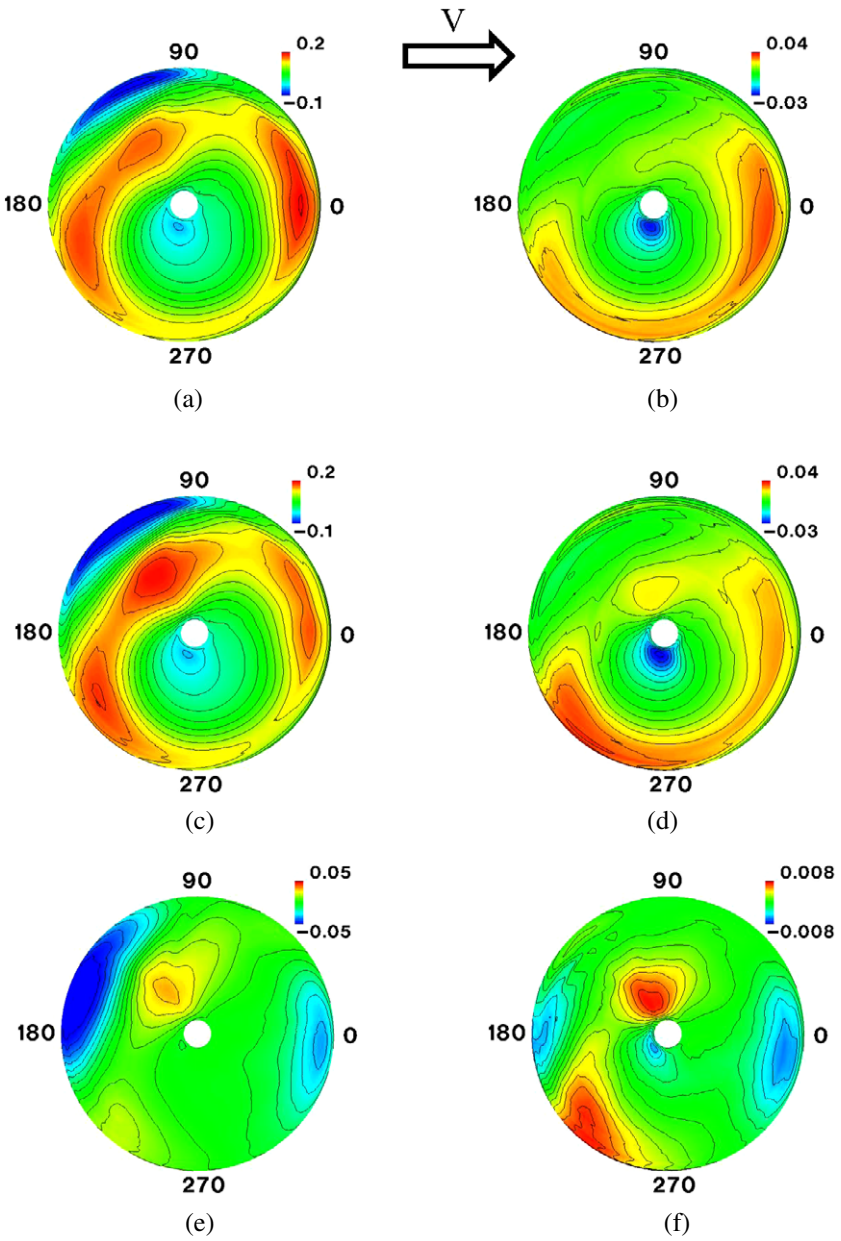

Figure 5. Rotor lift and drag distribution for the baseline and the soft rotor without TED. (a) M^2C_L, 100% GJ, (b) M^2C_D, 100%GJ, (c) M^2C_L, 50%GJ, (d) M^2C_D, 50%GJ, (e) ΔM^2C_L, 50%GJ − 100%GJ, and (f) ΔM^2C_D, 50%GJ − 100%GJ.

there is a decrease in drag. Overall, the performance of the rotor increases by about 2.3%.

Finally, the rotor disk loading for the stiff rotor with TED is shown in figure 8. The loading is shown with respect to the baseline stiffness with TED. Unlike the case of the soft rotor the lift on the front and aft increases and on the advancing and retreating side decreases. Correspondingly there is a decrease/increase in drag. Overall there is no appreciable change in performance.

6. Structural load analysis with CFD/CSD

This section examines the effects of torsion frequencies on the blade structural loads. The blade torsional stiffness variations are expected to have the largest impact on the blade torsion moments and pitch link loads and therefore only those quantities are investigated. Figure 9 shows the blade torsion moments at four radial locations (10%R, 30%R, 50%R, and 70%R) along the blade span for the soft (50%GJ), baseline (100%GJ), and stiff (150%GJ) rotor without TED, respectively. The results were obtained from the coupled CFD/CSD analysis. Detailed waveforms are slightly different among the three cases. However, the results show very similar magnitude. Figure 10 shows the same blade torsion moments for the 1/rev TED cases. Again, there are more similarities than differences among the three cases. Blade torsion moments show strong 1/rev variations similar to the 1/rev TED with 90° phase. The 1/rev TED increases torsion moment at 70%R.

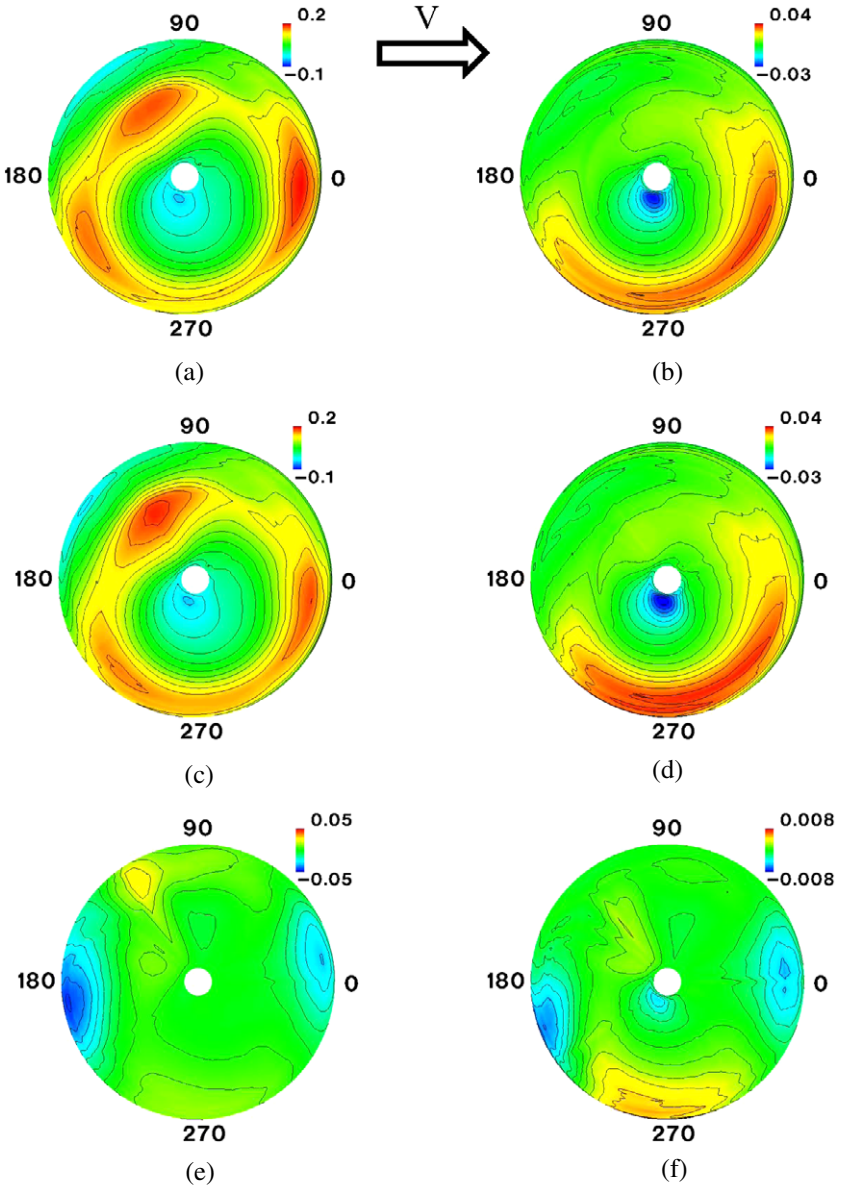

Figure 6. Rotor lift and drag distribution for the baseline and the soft rotor (50% GJ) with 1/rev TED. (a) M^2C_L, 100%GJ, (b) M^2C_D, 100%GJ, (c) M^2C_L, 50%GJ, (d) M^2C_D, 50%GJ, (e) ΔM^2C_L, 50%GJ − 100%GJ, and (f) ΔM^2C_D, 50%GJ − 100%GJ.

Figure 11 shows the peak-to-peak magnitude of torsion moments along the blade span. Again, the torsion frequency does not appear to have a significant influence on torsion moments. In the case of no TED, the peak-to-peak moment increases almost linearly as a function of the radial location from the tip to the root. The minimum peak occurs near 180° and the maximum peak occurs near 270° azimuth (see figure 9). Moving radially inboard from the tip to 30%R, the increase in the peak-to-peak magnitude occurs due to the decrease in the minimum peak at 180° azimuth, and further decrease moving from 30%R to the root occurs due to the increase in the peak-to-peak magnitude at 270° azimuth. Whereas in the case of 1/rev TED, the peak-to-peak moment increases from the tip to mid-span and then, unlike the no-TED case, remains relatively unchanged inboard of the mid-span to the root. This difference is due to the action of 1/rev TED which increases the torsion moment on the advancing side causing the maximum peak to occur at 90° azimuth (see figure 10) instead of 180° as in the case of no TED. Moving radially inboard from mid-span to the root, the 90° maximum increases while the 180° minimum also increases resulting in a relatively unchanged peak-to-peak magnitude. However, the 1/rev TED reduces torsion moments inboard and increases outboard around 70%R.

Figure 12 shows the calculated pitch link loads; both time history and peak-to-peak magnitude results. The waveforms are very similar between the baseline (100% GJ) and stiff (150% GJ) rotors for both without and with 1/rev TED. The same trend is observed for the peak-to-peak magnitude. The pitch link load magnitude is about 10% higher for the soft rotor. Also, for all the three rotor configurations, the peak-to-peak magnitude is slightly higher in the case of 1/rev

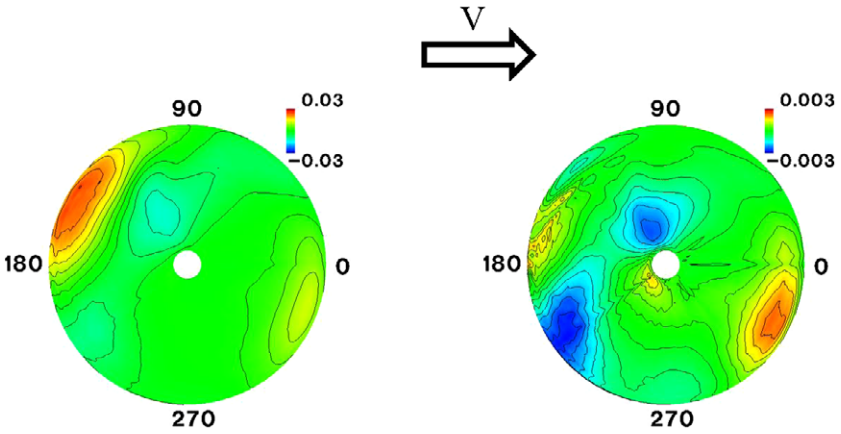

Figure 7. Rotor lift and drag distribution for the stiff rotor without TED. Loading is shown with respect to the baseline (100%GJ) case without TED. (a) $\Delta M^2 C_{\mathrm{L}}$, 150%$GJ$ − 100%GJ and (b) $\Delta M^2 C_{\mathrm{D}}$, 150%$GJ$ − 100%GJ.

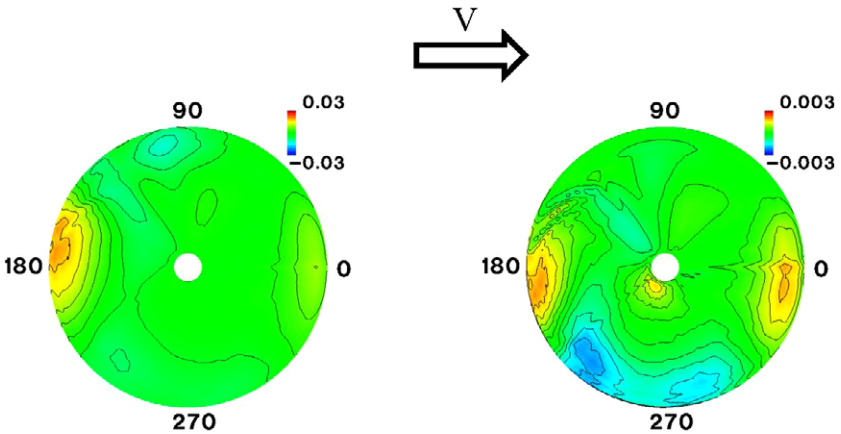

Figure 8. Rotor lift and drag distribution for the stiff rotor with 1/rev TED. Loading is shown with respect to the baseline (100% GJ) case with TED. (a) $\Delta M^2 C_{\mathrm{L}}$, 150% GJ minus 100% GJ and (b) $\Delta M^2 C_{\mathrm{D}}$, 150% GJ minus 100% GJ.

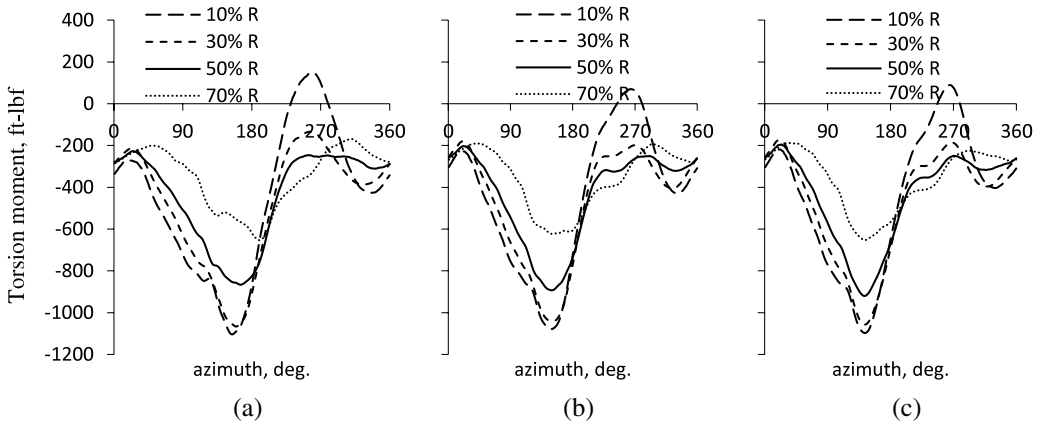

Figure 9. Torsion moment for the no-TED case. (a) 50% GJ, (b) 100% GJ, and 150% GJ.

TED relative to the no-TED case. The increase is due to the action of TED on the advancing side which significantly increases the torsion moments on the advancing side around 90° azimuth, as is also shown in figures 9 and 10.

7. Summary and Conclusions

In this study, the effect of variation of torsional stiffness on the performance and structural loads of a rotor without and

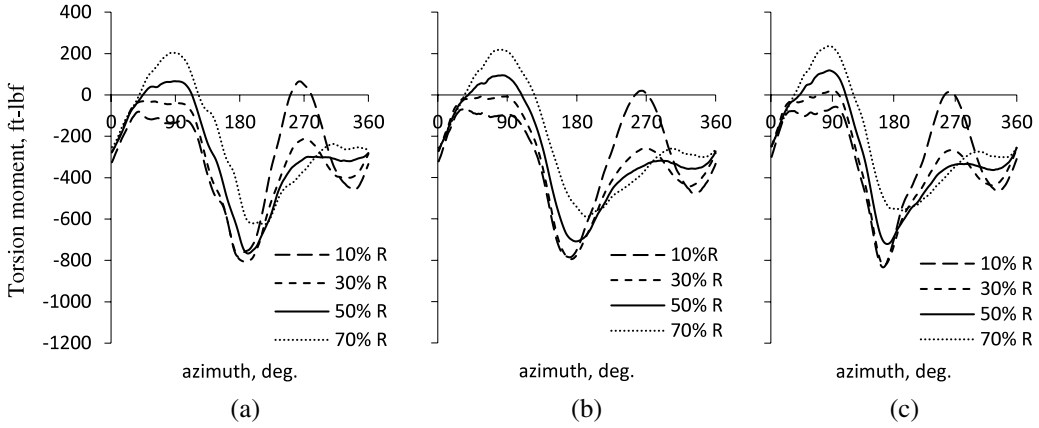

Figure 10. Torsion moment for the 1/rev TED case. (a) 50% GJ, (b) 100% GJ, and (c) 150% GJ.

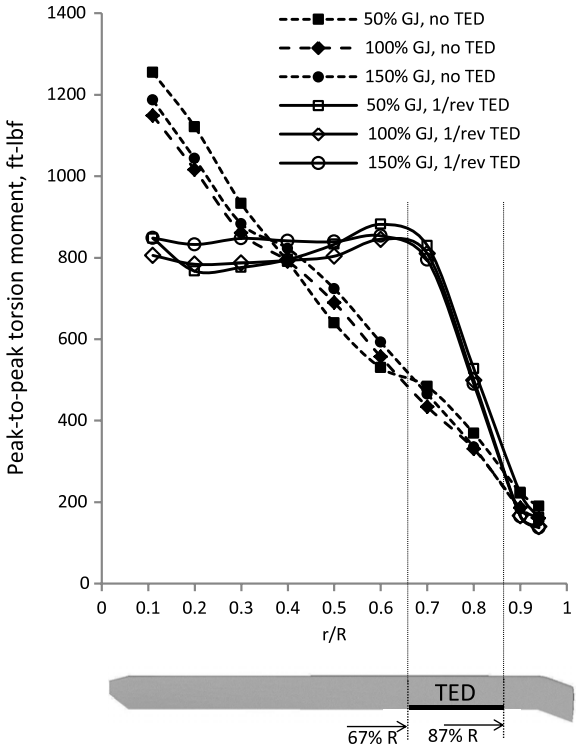

Figure 11. Effect of variation of torsional stiffness on peak-to-peak torsion moment.

with 1/rev TED is investigated. The UH-60A four-bladed articulated main rotor is studied at the high-speed forward flight condition. The blade torsional frequency is varied by modifying the spanwise torsional stiffness of the blade and/or the pitch link stiffness. The structural twist of the rotor blade, however, is not re-optimized as the torsional stiffness is varied but that of the baseline rotor is used for all the cases. Initially an exploratory study is carried out using the lifting-line comprehensive analysis on the soft and stiff rotors where phase and amplitude of the TED are varied and their optimum values are determined. Next, high fidelity coupled CFD–CSD simulations are carried out using the optimum phase and magnitude found with the comprehensive analysis. The results are compared with those of lifting-line calculations. The results in terms of the disk loading (M^2C_L and M^2C_D) are analyzed in order to understand the causes of apparent degradation or enhancements in performance as the stiffness is varied, both with and without TED motion. The effects of torsion frequencies on the blade structural loads are also examined. The following conclusions are drawn from the study.

(1) The blade torsion frequency plays a significant role in rotor performance. Design of active blades requires careful selection of blade torsion frequencies to produce good baseline rotor performance and sufficient control authority.

(2) Both lifting-line comprehensive analysis and coupled CFD–CSD simulation indicate that a soft rotor would incur a performance penalty. The penalty is significant, on the order of 6%, when TED is not applied. At this high-speed condition, the unsteady transonic pitching moment causes a large nose down pitch motion of the blade on the advancing side which incurs loss of lift and is the main cause of the calculated degradation in performance. In the case of TED, the penalty is only about 1%, as the application of TED counteracts the aerodynamic moments and reduces their effect.

(3) A stiff rotor resists the nose down pitching of the blade due to the pitching moments on the advancing side. In the case where TED is not present, the performance is slightly enhanced—the increase in performance is about 2.3%. In the case of TED, there is no appreciable change in performance compared to the baseline (100% GJ) case.

(4) With 1/rev TED, the peak performance achievable with the baseline stiffness cannot be significantly improved by changing the torsional stiffness.

(5) Variation of torsion frequency does not appear to have a significant influence on blade torsion moments, although the 1/rev trailing flap activation examined has an important role. For a soft rotor the pitch link load increases significantly compared to the baseline rotor whereas for a stiff rotor the pitch link load is relatively unchanged.

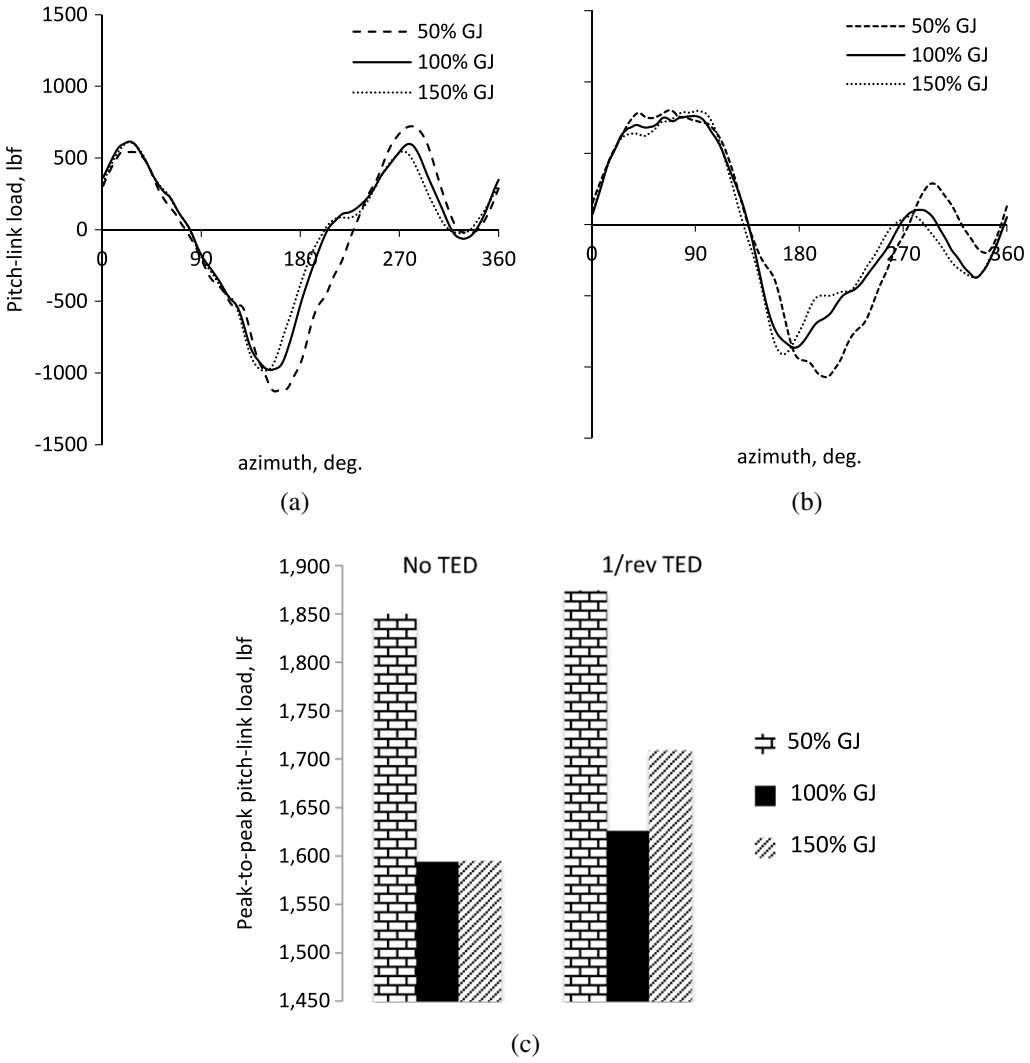

Figure 12. Pitch link load. (a) Baseline (no TED), (b) 1/rev TED, and (c) peak-to-peak variation.

Acknowledgments

This work was presented at the Future Vertical Lift Aircraft Design Conference, San Francisco, California, January 18–20, 2012. This work was performed while the first author was an employee at HyPerComp Inc. and was sponsored by US Army Research, Development, and Engineering Command (AMRDEC) under SBIR Contract# W911W6-08-C-0061. Technical monitors are Drs Hyeonsoo Yeo and Mark Fulton at the US Army Aeroflightdynamics Directorate (AFDD). This is a work of the US Government and is not subject to copyright protection in the US.

References

[1] Chopra I 2000 Status of application of smart structures technology to rotorcraft systems *J. Am. Helicopter Soc.* **45** 228–52

[2] Richter P, Eisbrecher H D and Klöppel V 1990 Design and first flight test of individual blade control actuators *16th European Rotorcraft Forum (Glasgow, Sept. 1990)*

[3] Jacklin S A, Blaas A, Teves D and Kube R 1995 Reduction of helicopter BVI noise, vibration, and power consumption through individual blade control *American Helicopter Society 51st Annual Forum Proc. (Fort Worth, TX, May 1995)*

[4] Norman T R, Shinoda P M, Kitaplioglu C, Jacklin S A and Sheikman A 2002 Low-speed wind tunnel investigation of a full-scale UH-60 rotor system *American Helicopter Society 58th Annual Forum Proc. (Montreal, June 2002)*

[5] Arnold U T P 2003 Recent IBC flight test results from the CH-53G helicopter *29th European Rotorcraft Forum (Friedrichshafen, Sept. 2003)*

[6] Norman T R, Theodore C, Shinoda P M, Fuerst D, Arnold U T P, Makinen S, Lorber P and O'Neill J 2009 Full-scale wind tunnel test of a UH-60 individual blade control system for performance improvement and vibration, loads, and noise control *American Helicopter Society 65th Annual Forum Proc. (Grapevine, TX, May 2009)*

[7] Yeo H, Romander E A and Norman T R 2011 Investigation of rotor performance and loads of a UH-60A individual blade control system *J. Am. Helicopter Soc.* **56** 042006

[8] Wilbur M L, Mirick P H, Yeager W T Jr, Langston C W, Cesnik C E S and Shin S J 2001 Vibratory loads reduction testing of the NASA/Army/MIT active twist rotor *American Helicopter Society 57th Annual Forum Proc. (Washington, DC, May 2001)*

[9] Riemenschneider J, Keye S, Wierach P and des Rochetter H M 2004 Overview of the common

DLR/ONERA project active twist blade (ATB) *30th European Rotorcraft Forum (Marseilles, Sept. 2004)*

[10] Sekula M K, Wilbur M L and Yeager W T Jr 2005 A parametric study of the structural design for an advanced active twist rotor *American Helicopter Society 61st Annual Forum Proc. (Grapevine, TX, June 2005)*

[11] Milgram J and Chopra I 1998 A parametric design study for actively controlled trailing edge flaps *J. Am. Helicopter Soc.* **43** 110–9

[12] Friedmann P P 2003 Vibration reduction in rotorcraft using actively controlled flaps—from theoretical concept to flight ready hardware *The Confederation of European Aerospace Societies/AIAA Joint International Forum on Strructural Dynamics and Aeroelasticity (Amsterdam, June 2003)*

[13] Shen J and Chopra I 2004 Aeroelastic modeling of trailing-edge-flap helicopter rotors including actuator dynamics *J. Aircr.* **41** 1465–72

[14] Fulton M V 2005 Aeromechanics of the active elevon rotor *American Helicopter Society 61st Annual Forum Proc. (Grapevine, TX, June 2005)*

[15] Straub F K, Anand V R, Birchette T S and Lau B H 2009 Wind tunnel test of the SMART active flap rotor *American Helicopter Society 65th Annual Forum Proc. (Grapevine, TX, May 2009)*

[16] Fulton M V 2000 Design of the active elevon rotor for low vibration *American Helicopter Society Aeromechanics Specialists' Mtg (Atlanta, GA, Nov. 2000)*

[17] Shen J, Chopra I and Johnson W 2010 Performance of swashplateless helicopter rotor with trailing-edge flaps for primary flight control *J. Am. Helicopter Soc.* **55** 042005

[18] Jain R, Yeo H and Chopra I 2010 Computational fluid dynamics–computational structural dynamics analysis of active control of helicopter rotor for performance improvement *J. Am. Helicopter Soc.* **55** 042004

[19] Kufeld R M, Balough D L, Cross J L, Studebaker K F, Jennison C D and Bousman W G 1994 Flight testing of the UH60A airloads aircraft *American Helicopter Society 50th Annual Forum Proc. (Washington, DC, May 1994)*

[20] Saberi H, Khoshlahjeh M, Ormiston R A and Rutkowski M J 2004 Overview of RCAS and application to advanced rotorcraft problems *American Helicopter Society 4th Decennial Specialist's Conf. on Aeromechanics (San Francisco, CA, Jan. 2004)*

[21] Jain R K, Ramakrishnan S V and Chen C L 2006 Enhancement of WIND-US for helicopter flow simulation *Paper No. AIAA-2006-3373, 36th Fluid Dynamics Conf. and Exhibit (San Francisco, CA, June 2006)*

[22] Chen C L, Chen Y C, Chen B, Jain R K, Lund T, Zhao H, Wang Z J, Sun Y, Saberi H and Shih T H 2007 High fidelity multidisciplinary tool development for helicopter quieting *Paper AIAA-2007-3807, 37th Fluid Dynamics Conf. and Exhibit (Miami, FL, June 2007)*

[23] Tung C, Cardonna F X and Johnson W 1986 The prediction of transonic flows on an advancing rotor *J. Am. Helicopter Soc.* **31** 4–9

[24] Potsdam M, Yeo H and Johnson W 2006 Rotor airloads prediction using loose aerodynamic/structural coupling *J. Aircr.* **43** 732–42

[25] Datta A and Chopra I 2008 Prediction of the UH-60A main rotor structural loads using computational fluid dynamics/comprehensive analysis coupling *J. Am. Helicopter Soc.* **53** 351–65

[26] Nygaard T A, Saberi H, Ormiston R A, Strawn R C and Potsdam M 2006 CFD and CSD coupling algorithms and fluid structure interface for rotorcraft aeromechanics in steady and transient flight conditions *American Helicopter Society 62nd Annual Forum Proc. (Phoenix, AZ, May 2006)*

[27] Jain R, Yeo H and Chopra I 2010 Examination of rotor loads due to on-blade active controls for performance enhancement *J. Aircr.* **47** 2049–66